Force Measurement Techniques for Hypersonic Flows in Shock Tunnels

Niranjan Sahoo[*,1], **and K.P.J. Reddy**[†]
[*]Department of Mechanical Engineering, Indian Institute of Technology Guwahati, Guwahati – 781 039, INDIA.
[†]Department of Aerospace Engineering, Indian Institute of Science, Bangalore – 560 012, INDIA. Phone. 0091-80-22932758, Fax. 0091-80-23606223, 23600134, E-mail. laser@aero.iisc.ernet.in

Abstract
Recent advances in hypersonic research activities have led to the development in ground based test facilities for simulating near-realistic flight conditions in the laboratory. Basic performance data such as drag, lift, thrust etc., are usually obtained from ground-based experimentation for physical understanding of the flow fields and subsequent prototype developments. Hypersonic flows are produced for a very short time in impulse facilities such as shock tunnels, free-piston shock tunnels and expansion tubes. The test times are in the order of few milliseconds in the shock tunnel and for the expansion tubes, it is still less (~50 μs). The force measurements in these facilities are very challenging due the need of fast response sensors and instrumentations. In this review paper, two force measurement techniques are discussed that are best suited for short duration facilities namely; accelerometer balance and stress-wave force balance system.

Keywords: Impulse facilities, hypersonic flow, accelerometer balances, stress-wave force balance.

1. INTRODUCTION

The term 'hypersonic' is used to describe a flow where the flight velocity is much greater than the ambient speed of sound. The distinguishable features that characterize hypersonic flow fields are thin shock layers, thick boundary layers, strong entropy layers, dominating viscous interaction, regions of strong vortices, low density flows and high temperature effects (Anderson 2006). Over the last few decades, there has been resurgence of interest in hypersonic flow due to considerable research and developments of single-stage-to-orbit (SSTO) vehicle, aero-assisted orbital transfer vehicle (AOTV), re-entry vehicles, hyper-X experimental plane, hypersonic reusable vehicles and scramjet technologies (Bertin and Cumming 2003; Stalker *et al* 2005). The success of future hypersonic flights demands clear understandings of high-speed flow physics and various performance parameters of the flight. One of the major studies includes accurate prediction of aerodynamic forces/moments which is necessary for vehicle stability, guidance/control system and landing characteristics of the flight.

A more realistic approach to understand the hypersonic flow physics would be to simulate the flight conditions in the laboratories. During the 1960's considerable research was conducted to establish ground test facilities to simulate supersonic and hypersonic flows. Mainly, the research was focussed at understanding the problem of re-entry and to generate aerodynamic data for simple geometries such as cones/slender bodies. Analytical models were developed to validate the data for understanding aerodynamic behaviour (Van Dyke 1958; Charles and Merle 1962). But, due to lack of availability of high speed sensors and flow diagnostic instrumentation, these facilities provided limited data. With

[1]Corresponding Author: Dr. Niranjan Sahoo, Associate Professor, Department of Mechanical Engineering, Indian Institute of Technology Guwahati, Guwahati – 781 039, INDIA. Phone. 0091-361-2582665, Fax. 0091-361-2690762, E-mail. shock@iitg.ernet.in

advent of computational power, the new era of hypersonic relies heavily on CFD codes to simulate flow parameters for complex aerodynamic body shapes. Again, validation of these codes against experimental test plays a vital role to understand flow phenomena and subsequent numerical code development. So, ground-based experimentation in high-speed ground test facilities remains an important component for future developments in hypersonic vehicles.

Hypersonic flows are produced for a very short time in impulse facilities with test times in the range of 0.05-10 ms. So, the aerodynamic testing in these facilities is considered as highly specialized activity. These facilities include small and large scale developments in shock tunnels, free-piston shock tunnel and expansion tubes over last few decades (Modarres and Azzazy 1988; Lu and Wilson 1994; Doolan and Morgan 1999; Itoh *et al* 2001). Main attraction of short duration facilities is that they provide a high-enthalpy slug of test gas at reasonable cost. The test gas is compressed and subsequently expanded with appropriate nozzle to achieve desired conditions in the test section of the tunnel. Though, there are difficulties in the process of data acquisition in the short test times, but the modern days of high-speed instrumentation and flow diagnostics techniques have produced ingenious solutions to take the advantage of short test times.

The aerodynamic forces and moments on a body moving in air are due to two basic sources i.e. pressure and shear stress distribution on the surface of the body. The pressure acts normal to the surface whereas the shear stress acts tangential to the surface. The net effect of pressure and shear stress integrated over the complete body surface is the resultant aerodynamic force and moment on the body. One way to obtain the forces and moments on the model is by measuring local pressures and then integrating it on the model surface (indirect measurement). The other way is to measure the forces/moments directly with appropriate sensors and instrumentation (direct measurement).

One of the methods of *indirect* force measurement technique is by pressure sensitive paints (PSP). These paints have the potential for measuring instantaneous two-dimensional pressure distributions on a model surface exposed to aerodynamic flows. It allows the quantitative estimate of absolute pressures at any desired location on the model surface without disturbing the flow field and distorting the model surface. The aerodynamic forces and moments are then obtained by integration of pressure data, over the certain desired area on the model surface. The concept of surface pressure field measurement using PSP methodology was brought into limelight worldwide in mid-1980s by Ardasheva et al (1985). Further efforts on this technology for a various aerospace applications have been introduced in low speed wind tunnels (McLachlan *et al* 1992; Gallery *et al* 1994), low speed flows in Boeing commercial airplane (Dale *et al* 1998) and flight test (McLachlan *et al* 1992; Houck *et al* 1996). Although few attempts have been made to use PSP in short duration hypersonic flows in shock tubes/tunnels, but they are not intended for inferring aerodynamic forces from the measured signals. (Jules *et al* 1995; Hubner *et al* 2000; Hubner *et al* 2001). It is mainly due to the fact that high enthalpy hypersonic flow over the model produces significant increase in temperature and skin friction on the model surface. Most of the available PSPs have limitations withstanding such high pressure/temperature gradients. The response time for these paints are high compared to its counterparts such as pressure transducers. Also, there are associated difficulties in pressure mappings during acquisition of data. Another indirect approach for developing a mechanism to measure short-duration forces and moments in continuous-flow tunnels is based on the measurements from accelerometers and strain gauges (Marqart and Coulter 1998). It involves marrying accelerometers with standard force and strain gauge balances to produce an instrument that has both frequency response of accelerometers and the operational efficiencies of wind-tunnel balances. The short duration normal forces are then calculated by adding together the information from accelerometers and strain gauges. The impulse is the integration of short-duration force with respect to time over the time of pulse duration.

The other way is to measure the forces/moments directly with appropriate sensors and instrumentation (direct measurement). In particular for hypersonic flows in shock tunnels, the response time for these sensors must be much smaller than the test flow duration available in the facility. Hence, obtaining forces and moments by integrating local pressure measurements is extremely expensive in

terms of model complexity and testing time for realistic model shapes and cannot provide a measure of viscous contributions. In this paper, two major techniques of force balance system are discussed that are mainly used in shock tunnels i.e. accelerometer balance systems and stress-wave force balance systems. Before focussing the attention to these techniques, a brief history of some conventional methods of direct force measurement techniques attempted by researchers in high speed flows are discussed.

2. CONVENTIONAL FORCE MEASUREMENT TECHNIQUES: A BRIEF HISTORY

The comprehensive review on *direct* force measurement techniques used in impulse facilities has been well-documented in the open literatures (Bernstein 1975; Simmons 1995). These force balances are based on two modelling assumptions. The first type of balances are known as *inertia-dominated force balances* in which members of force balance structure are considered as lumped parameter elements. In the second category, the forces are measured by treating the model to behave as a rigid body. These balances are called *stiffness-dominated force balances*.

Inertia-dominated balances rely on measuring the components of acceleration during free flight of the model in the test section. With prior knowledge of mass and moment of inertia, it is possible to calculate aerodynamic forces and moments by measuring the model acceleration. However, the free flight movement is achieved momentarily for few milliseconds. Several methods has been devised in the past to release the model in the test section such as fuse-wire technique (Lam and Stollenwerk 1966), split hallow shell (McDevitt and Larson 1966), inverted pea shooter (Platou 1968) and energy transmission technique (Wyborny and Requardt 1974). During free flight movement, optical tracking systems with high speed photography (Lam and Stollenwerk 1966; McDevitt and Larson 1966; Platou 1968; Wyborny and Requardt 1974; Strawa *et al* 1991), laser interferometry (Bernstein and Stott 1982), photo-detector sensitive light beam (East and Hillier 1985) techniques are used to record the flight path. Then, the model accelerations are deduced by differentiating the flight path twice. With subsequent developments in transducer technology, accelerometers are mounted on the models to measure accelerations directly. A novel free-flying technique has been developed by Naumann *et al* for releasing the model during the test flow and measuring accelerations directly using accelerometers (Naumann *et al* 1991; Naumann *et al* 1993). This technique is a combination of fixed and free flying model technique. The model is fixed in position with a stem in the test section. A fast acting mounting support releases the model just before the onset of the flow and grips it again after free flight duration (1-2 ms) is over.

In the second category i.e. stiffness dominated force balances for impulse facilities (test times less than a millisecond), the model is attached to the balance system as a linkage through beam elements where strain gauges are located (Jessen and Gronig 1989; Carbonara 1993; Storkmann *et al* 1998). When the model experiences the forces, the aerodynamic loads are transmitted to the beam element. Depending on the magnitude of forces, strain gauges are deformed and deliver force-proportional signal through a Wheat-stone bridge circuit integrated with the strain gauges. However, the force measurements require either an acceleration compensation of measured data or a stiff construction of the balance. The main advantage of a stiff construction is that the measurements and its evaluation become independent of the model. In this context, “stiff” means that at least 5-cycles of the lowest natural frequency of the model-balance-sting system should be observed within the test time i.e. for a test time of typically 5-millisecionds in a shock tunnel, a lowest natural frequency of 1 kHz is required. Higher is the natural frequency, better is the justification for neglecting acceleration compensation. In earlier days, the strain gauge technologies were limited and the natural frequency of model-balance system restricted the stiffness dominated force balances to yield measurable strains. With the refinement of the high-sensitivity semiconductor strain gauges, Jessen and Gronig (1989) introduced a model in combination with a high stiffness and low moment of inertia balance fitted with semiconductor strain gauges to design a six-component force balance for shock tunnel application. In order to include the effects of vibrations associated with bending and pitching motion of the sting, the inertia forces with variations of low frequencies are compensated by measuring accelerations at various locations (Holden 1985; Storkmann *et al* 1998; Itoh *et al* 2001).

3. IMPORTANT CONSIDERATIONS FOR FORCE BALANCES IN IMPULSE FACILITIES

It is a well known fact that environments associated with hypersonic test facilities (such as shock tunnels) are harsh, both inside and outside the test facility. Inside, the measurement environment is characterized by high temperatures, high velocities and high noise levels. Outside, it is characterized by high noise and vibration levels. Hence, the accuracy level of measurements in the shock tunnel is mainly coupled with the instruments involved in the facility. A more important criterion regarding the measurement requirement is the duration of the flow where the type of instrumentation, frequency response and measurement durations are dictated by the test facilities (Rogers and Mason 1966; Modarress and Azzazy 1988).

Hypersonic steady flows in the test sections of impulse facilities are generated for a very short test times. In shock tunnels, this time is of the order of few milliseconds whereas in expansion tubes the hypersonic flows prevail only for about 50 μs. So, during the short period of steady flow, no steady state force equilibrium can be achieved between the model and its support. In the case of force measurement with inertia-dominated balances, the model is momentarily in free flight in the test section. The flight paths are measured by optical tracking system during test flow duration and then differentiated twice to measure the acceleration. Although this method is insensitive to nonlinearities/disturbances in the flow, but it needs the synchronization of model release mechanism and optical tracking system exactly during the test flow. When stiffness dominated balances are used, the sensitivity of the strain gauges plays a vital role in inferring the data along with the acceleration compensation. The forces to be measured, is produced by external aerodynamic load as well as due to inertia effects of the model and support. This becomes more complicated, if aerodynamic load history is not linear or unpredictable particularly at the starting phase of the tests with models of complex geometries.

Based on the considerations and with the availability fast response strain gauges, piezeofilms and accelerometers, it is possible to measure the aerodynamic forces by interpreting the signals from the instruments. Depending on the sensors used, they are called as accelerometer balance or stress-wave force balance system.

4. ACCELEROMETER BALANCE SYSTEM

The accelerometer balance system in a shock tunnel is based on measuring transient accelerations of the model during the period of steady tunnel flow. The force measurement is achieved through direct measurement of accelerations by mounting model through a flexible support so that it can be considered as 'unrestrained' during the flow duration. Such a balance system is instrumented with number of commercially available accelerometers to sense the accelerations. For shock tunnels, this fixed model technique was first designed and demonstrated experimentally by Vidal (1956). He proposed to replace the model and its support with a single degree of freedom spring-mass system, acted upon by an unsteady force. The displacement, velocity and acceleration of the mass can be written as;

$$\text{Displacement, } \chi(t) = \frac{1}{m\omega}\int_0^t F(\tau)\sin\omega(t-\tau)\,d\tau \tag{1}$$

$$\text{Velocity, } v(t) = \frac{1}{m}\int_0^t F(\tau)\cos\omega(t-\tau)\,d\tau \tag{2}$$

$$\text{Acceleration, } a(t) = \frac{F(t)}{m} - \omega^2\chi(t) \tag{3}$$

where, m is the mass of the body, $F(t)$ is the applied force, $\omega = \sqrt{\frac{k}{m}}$ is the natural frequency of the system, k is the spring constant, t is the time and τ is the dummy variable of integration.

It is observed that the acceleration equation (Eq. 3) is an algebraic function of the applied force and displacement at any time (t). Thus, it is possible to determine the applied force from the acceleration and displacement measurements from the simple equation of motion, i.e.

$$F(t) = m\left[a(t) + \omega^2 \chi(t)\right] = m\left\{a(t)\right\} + k\left\{\chi(t)\right\} \tag{4}$$

Further approximation in Eq. (4) can be made by assuming sufficiently small elastic restraint for which the spring force can be neglected while determining the applied force on the model. Then, the model becomes completely unrestrained and will be a free body acted upon, only by the aerodynamic forces. This elementary analysis leads to a conclusion in inferring time-dependent aerodynamic forces by direct measurement of model acceleration. With respect to shock tunnel applications where the model experiences a constant force during steady flow duration, the model equation of motion can be further simplified as;

$$\text{Acceleration, } a(t) \approx \frac{F}{m} \tag{5}$$

$$\text{Velocity, } v(t) \approx \frac{F}{m} \cdot t \tag{6}$$

$$\text{Displacement, } \chi(t) \approx \frac{F}{m} \cdot \frac{t^2}{2} \tag{7}$$

Since, both the velocity/displacements are initially zero and grow with time; so, they introduce errors into the measurement. In contrast, the acceleration attains the maximum value initially and decreases slightly after a relatively long time interval. Thus, it is more desirable to determine the

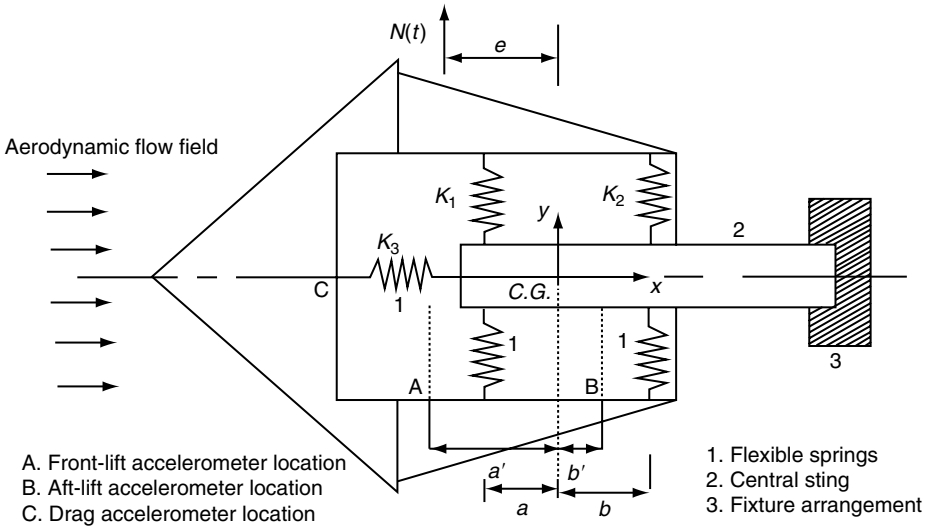

Figure 1. Spring-mass system for a three-component accelerometer balance mounted internally to a hallow model.

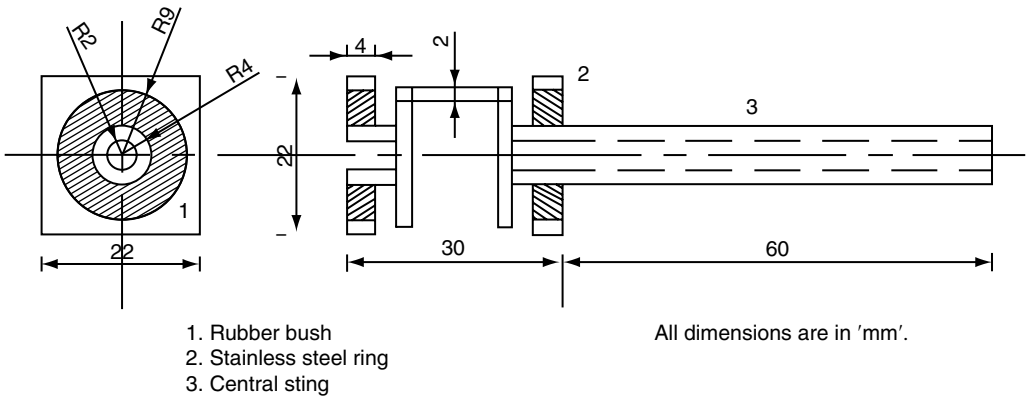

Figure 2. Accelerometer balance system with flexible rubber bushes (Sahoo *et al* 2007).

applied force from acceleration measurements. Vidal (1956) proposed a fixed model technique with springs in combination with acceleration sensing units for the force balance system in the shock tunnel as shown in Fig. 1. It was pointed out that aerodynamic forces could be measured with 98% accuracy in millisecond flow duration by neglecting the spring forces. This analysis was further extended for standard values of spring constants and certain model parameters for shock tunnel applications by estimating *zero-crossover time* (how fast the peak acceleration response drops to zero and becomes negative) and percentage of drop in normal and axial acceleration within a time domain of one millisecond (Sahoo *et al* 2003; Sahoo *et al* 2007). It was observed that higher values of spring constants have detrimental effects on the model accelerations even for short test flow duration. So, while dealing with measurements in shock tunnels and to get better accuracy in measurements through spring suspension, the spring constants should be chosen judiciously.

Though, the preceding discussions indicate that spring suspension system is ideal for an accelerometer balance system, but there are difficulties in mounting the model with the help of springs. So, the springs have to be replaced by a more realistic soft suspension system that essentially gives rise to negligible effects on model acceleration during test time scale. One of the methods has been proposed to mount the integrated model-balance system by flexible rubber bushes to achieve the free movement of the model in the test section particularly during the test flow duration (Sahoo 2003; Sahoo *et al* 2003). Another novel method to achieve the unrestrained motion is to mount the model-balance system by frictionless (Joarder and Jagadeesh 2004). Figure 2 shows, an accelerometer balance system mounted internally with flexible rubber bushes, where as the balance system with frictionless roller bearing is shown in Fig. 3. In both the realistic methods, the analytical spring-mass system of equations fail to include the inertia effects of the support on the model acceleration due to sudden aerodynamic load on the model. So, the performance of an accelerometer balance system is evaluated by finite-element modeling of the integrated model balance system (Sahoo 2003; Sahoo *et al* 2003; Joarder and Jagadeesh 2004).

4.1. Finite Element Analysis of Accelerometer Balance System

With recent advances in high speed computing facilities, the finite-element method has become a powerful tool for the numerical solutions in wide range of engineering problems. In this method of analysis, a complex region defining a continuum is discretized into simple geometric shapes called finite elements (FE). The material properties relating the deformations, stresses and the governing relationships are considered over these elements and are expressed in terms of unknown variables at the element nodes. An assembly procedure, duly considering the element boundary conditions (in terms of displacements or forces) and constraints, result in a matrix equation, which is called the equilibrium equation. Solution of this equation gives us the approximate behavior of the continuum in a piece-wise continuous sense. Therefore, as the discretization of the domain is made finer with smaller element size,

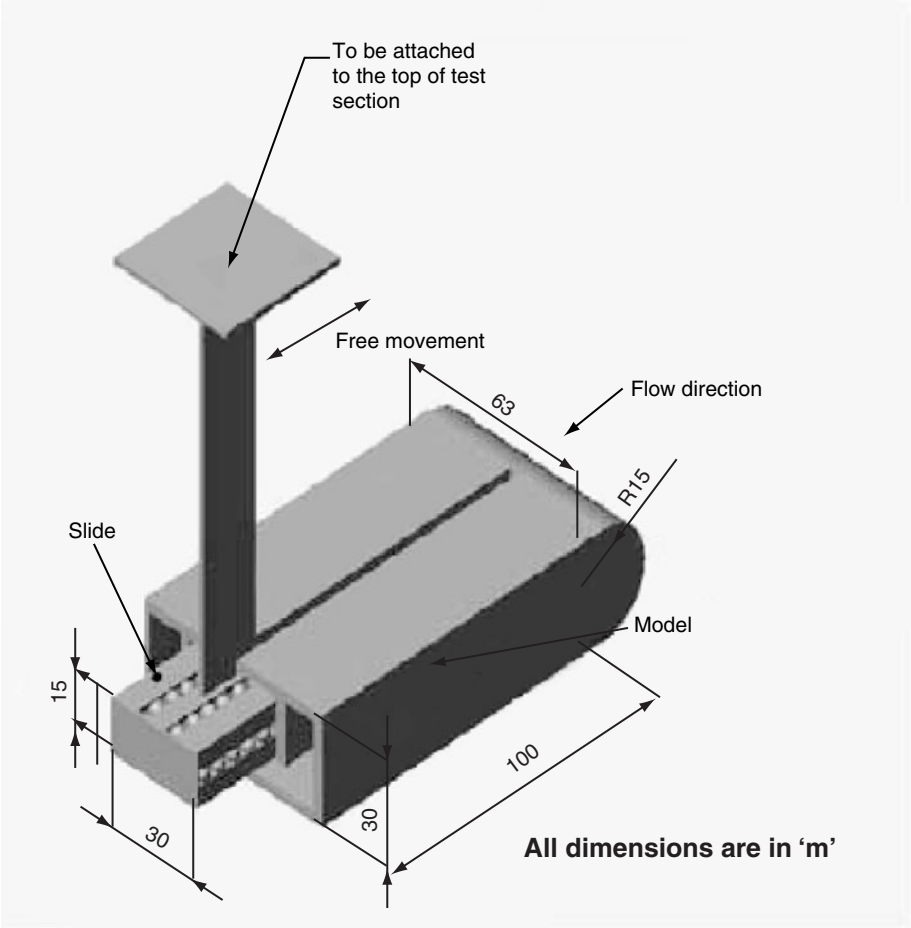

Figure 3. Accelerometer balance with roller bearings (Joarder and Jagadeesh 2004).

the energy of the system is equilibrated more accurately, and the result converges to the almost exact solution. In particular, the FE method is particularly useful in dynamic analysis, where exact analytical solutions are extremely difficult to obtain, and simply not tractable for complex problems involving arbitrary geometry and time-dependent boundary conditions.

Dynamic analysis involves the analysis of the model subjected to time-varying loads. There are four basic components of a dynamic system; stiffness (spring), inertia (mass), coefficient of damping (damper), and applied load. When a particular structure responds to an applied dynamic load, the system variables (e.g. displacements, velocity) are functions of the system characteristic response as well as the frequency and amplitude of the applied load. The governing equation for dynamic analysis in general matrix form is represented as (Sahoo 2003):

$$[M]\{\ddot{U}\} + [C]\{\dot{U}\} + [K]\{U\} = \{F(t)\} \tag{8}$$

where $[M]$ is the mass matrix of the active degrees of freedom, $[C]$ is the damping matrix, $[K]$ is the stiffness matrix of the structure, $\{U\}$ is displacement vectors (and derivatives are with respect to time) and $\{F(t)\}$ is the time varying applied loads. The left hand side of the equation represents the internal forces while the right hand side specifies the external forces. The general solution is finally obtained by satisfying the initial conditions ($t = t_0$) for $\{U(t_0)\}$ and $\{\dot{U}(t_0)\}$. There are two approaches adopted for general solution (Bathe 1997); one of the procedures is to transform the time-dependent problem

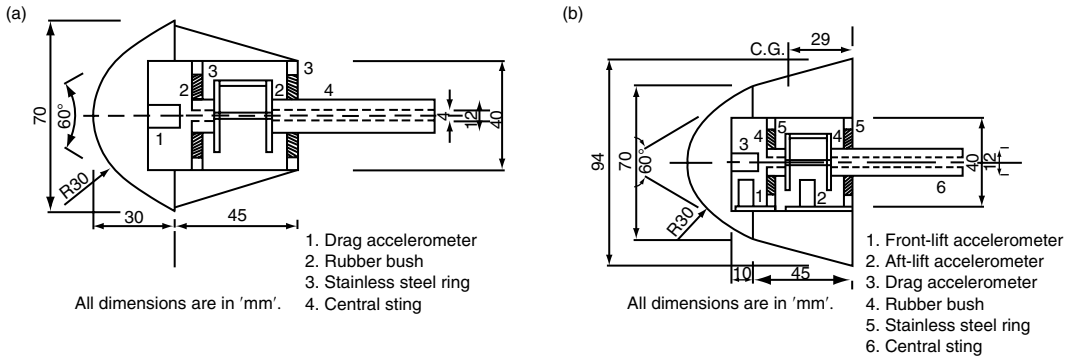

Figure 4. Blunt cone model mounted with accelerometer balance with flexible rubber bushes: (a) without an aft-body; (b) with a flare as an aft body (Sahoo 2003).

into a frequency-dependent psudo-static problem which is known as "modal analysis". The other procedure is to integrate the system (Eq. 8) directly through appropriate time-integration scheme. This time-integration scheme can lead to a most general approach, particularly suited for problems involving very small time-scale.

In particular, when the model is subjected to aerodynamic shock, stress waves are generated in the body that creates abrupt changes in stresses that travel through a material. A FE model of this process is limited in its frequency content by the size of the largest elements. One way to capture all the important wave modes, including those at high frequencies, is to use a sufficiently high cutoff frequency to obtain enough solution accuracy. The most accurate solution is obtained by integrating with a time step equal to the stability limit and the solution is less accurate when a smaller time step is used. So the optimal time step is again related to frequency of wave propagation and the FE size (Bathe 1997). For optimal analysis, the FE size should be kept between $\lambda/6$ to $\lambda/4$, where λ is the critical wavelength. Hence, handling aerodynamic shock loading needs judicious choice of the FE mesh and time step for analysis and accurate prediction of the design variables. On the basic of FE analysis frame work with the help of commercial package NISA, two major types of suspension system (one with flexible rubber material and the other with frictionless rollers) for an accelerometer force balance system have been reported in the literatures (Sahoo 2003; Sahoo *et al* 2003; Joarder and Jagadeesh 2004).

Flexible Rubber Material Suspension System: For blunt cone models, a three-component accelerometer balance system made out of annular stainless steel rings is directly mounted inside the model are shown in Fig. 4. It has two annular rubber bushes adhesively bonded with the outer ring as well as a sting. The sting is attached to the fixture arrangement in the test section. One accelerometer is screwed along the model axis to measure drag and two accelerometers are mounted on the base plate at appropriate places for measuring the normal forces. This base plate in turn is fitted to the annular ring as shown in Fig. 4-b. A more realistic approach to this accelerometer balance system is to study the system dynamics of model-balance assembly due to sudden aerodynamic load with finite element techniques. Accordingly, suitable rubber bushes can be selected so that model can be supported in the test section and its acceleration history within the experimental time scale will be almost independent on the inertia of the integrated system. An important study has been conducted through axi-symmetric FE simulation for a blunt cone model to quantify the rubber material by its Young's modulus (Sahoo *et al* 2003; 2007). The axi-symmetric finite-element for the model under consideration is shown in Fig. 5-a. From this analysis, it is concluded that standard neoprene rubber with Young's modulus of 300MPa is ideal for test flow duration of 1ms because, there is not significant drop in model acceleration during this period. The other interesting outcome of this analysis is the comparison of the simulated time history of acceleration with experimentally measured signal from the accelerometer mounted along the axis of the model (Fig. 6). Because of axi-symmetric formulations, the FE simulation could not predict effects rubber properties on normal acceleration for the model at angles of attack.

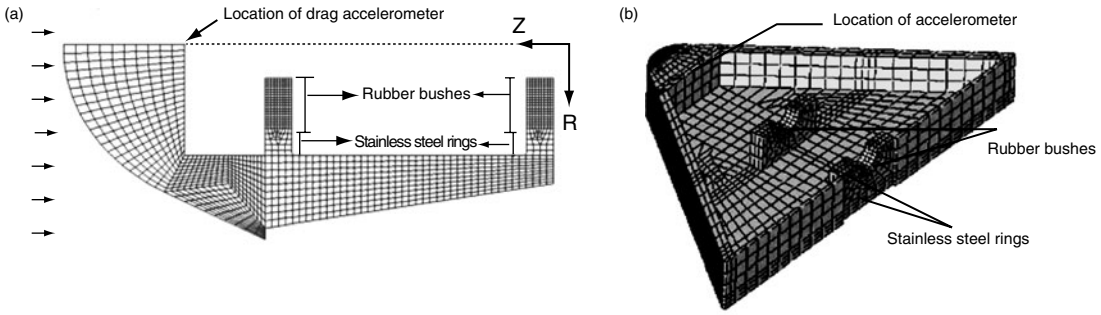

Figure 5. Finite-element mesh for the models: (a) axi-symmetric mesh for the blunt cone model (Sahoo *et al* 2003); (b) three-dimensional mesh for blunt-nosed triangular plate (Sahoo *et al* 2007).

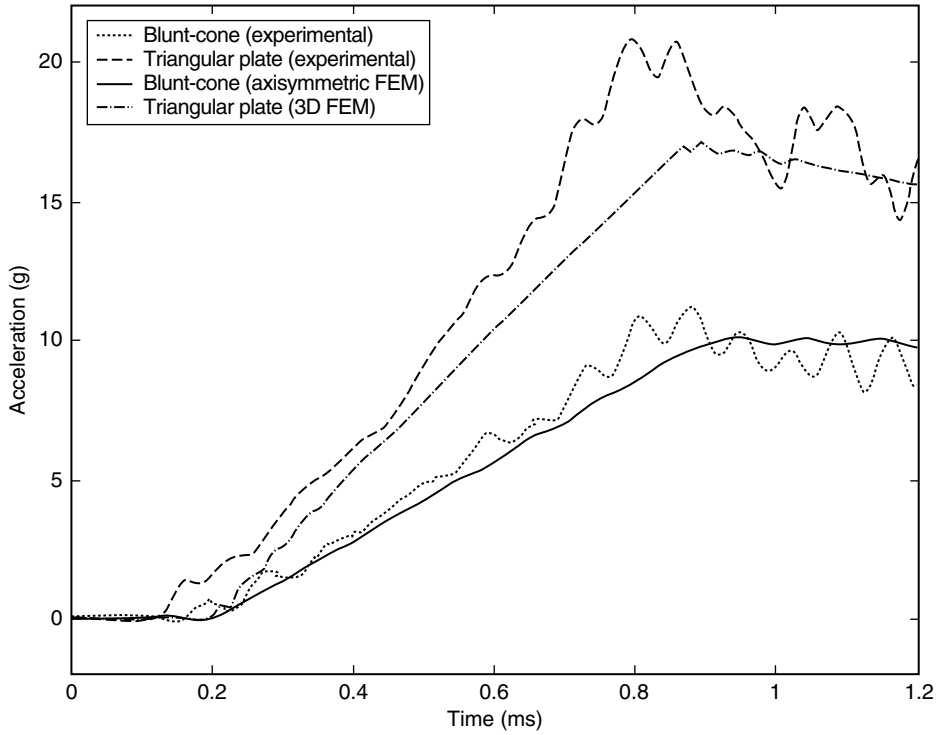

Figure 6. Comparison of measured model acceleration with finite-element simulation for flexible rubber bushes (Sahoo *et al* 2007).

Another similar study on accelerometer balance system based on three-dimensional FE analysis of mounting system with rubber bushes has also been reported (Sahoo *et al* 2007). In this case, a thin flat balance (Fig. 2) is housed inside a blunt-nosed triangular plate model. The balance system is made out of stainless steel rings with square cross section and adhesively bonded with outer annular rings as well as with the a sting and the corresponding FE model of the integrated assembly is shown in Fig. 5-b. Effects of rubber stiffness on acceleration history at 0° angle of attack is studied that again shows that the Young's modulus (E) of 0.3-3 MPa rubber is ideal for test time duration of 1 ms (Fig. 7). Measured acceleration during a shock tunnel test at 0° angle of attack compares well with FE simulation (Fig. 6). Although, the three-dimensional FE model is capable of predicting the balance performance at angles of attack, but due to lack of experimental data no further literatures in this direction has been reported.

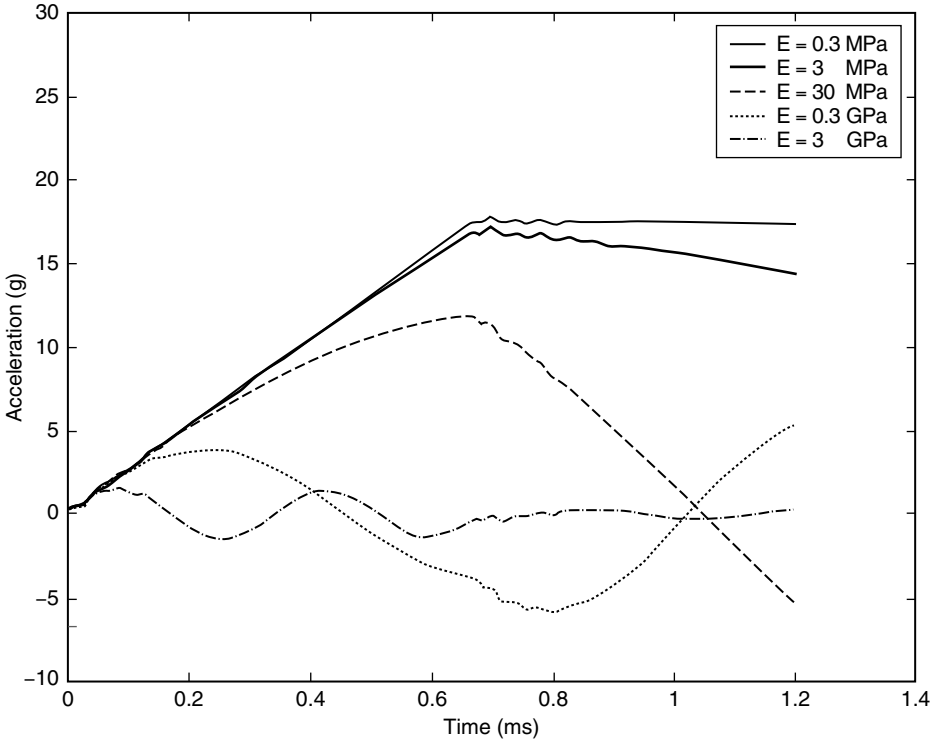

Figure 7. Effect of rubber stiffness on model acceleration history (Sahoo *et al* 2007).

Frictionless Roller System: A new free floating accelerometer balance system using frictionless rollers has been developed to measure drag on a blunt leading edge flat plate in IISc hypersonic shock tunnel (Joarder and Jagadeesh 2004). The schematic diagram of the balance system along with the model is shown in Fig. 3. In this case, the model is free to move on the steel slide block with spherical grooves on the top and side surfaces. Steel rollers inserted into these grooves ensure point contact between the model and slide. A steel strip with chamfered edges connects the slide from the roof of the test section. Thus, one end of the slide remains fixed during the test while the model moves in the axial direction with certain velocity depending on its mass and free stream conditions during testing. An accelerometer mounted along the axis measures the model acceleration. A three-dimensional finite element study of the model-balance is carried out by applying a force history prevailing in the test section. The time history of model acceleration from FE simulation is compared with the measured accelerometer signal (Fig. 8).

4.2. Force Measurement with Accelerometer Balance

The accurate measurement of aerodynamic forces from an accelerometer balance system mostly depends on the calibration that includes;

- selection of the suspension system for model-balance assembly and thereby ensuring free movement of the model during test time (discussed in section 4.1)
- estimation of model parameters and selection of accelerometer (Sahoo 2003)

The selection of support system is mainly decided, depending on the type of applications. In order to study the external aerodynamics on the model surface, standard neoprene type of rubber materials are mainly used for supporting the model and balance. In many applications such as scramjet engines, internal aerodynamics is more important to measure drag and thrust of the engine. So, it is desired to

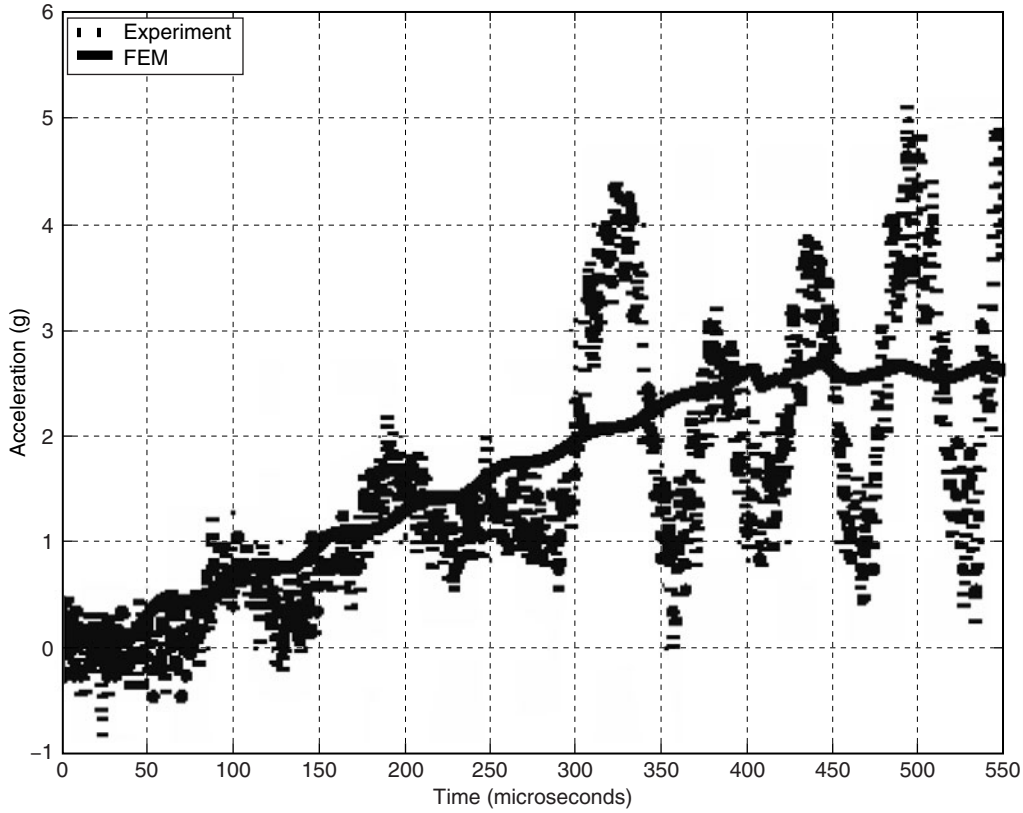

Figure 8. Comparison of measured model acceleration with finite-element simulation for roller bearing support (Joarder and Jagadeesh 2004).

support the model externally through the roller bearing suspension. In both the arrangements, the prime objective is to achieve the free movement of the model during test flow. The duration of unrestrained/free movement of model for a particular type of suspension system can be predicted by finite element analysis of model-balance assembly as discussed in earlier sections. During experiment, model accelerations are measured using accelerometers (Model M303A; PCB Piezotronics, USA) that are directly procured from the manufacturer (Sahoo 2003). The important factors pertaining to accelerometer selection are its size/dimension, sensitivity, usable frequency range and linearity. Although the sensitivity is supplied by the manufacturer, static calibration using standard accelerometer kit (Model 4294; Bruel & Kjaer, Denmark) has been performed (Sahoo 2003). Dynamic calibration with impact hammers (Model 208A03; PCB Piezotronics, USA) for accelerometers has also been reported (Joarder and Jagadeesh 2004). Both static and dynamic calibration of accelerometers under experimental domain can increase the accuracy level of force measurements in shock tunnels. Estimation of other model parameters, such as location of centre of gravity, center of pressure and moment of inertia, are mainly required for lift and pitching moment measurements and they can be found out experimentally (Sahoo 2003).

Once free movement of the model is ensured, accelerometers mounted at appropriate locations can be used with confidence to measure model accelerations within test time scale. For single component balance, only one accelerometer mounted along the model axis is sufficient for measuring drag even at angles of attack. When it is desired to measure lift and moments on a model, at least two accelerometers are required on either side of the center of gravity (CG) to infer the model accelerations. Although, a single accelerometer located at CG can measure the normal accelerations, but there are practical

difficulties in mounting the accelerometer exactly at CG. Moreover, when the size and mass of the model increases, single accelerometer located at CG may not infer complete information about the model movements. So, a three-component accelerometer balance has two lift accelerometers mounted on either side of CG for measuring the resultant model acceleration at angles of attack (θ). The normal force (N_t), axial force (C_t) and location of center of pressure (e) are then calculated from the measured accelerations as (Vidal 1956);

$$N_t = \frac{m_m(b'\xi_2 + a'\xi_3)}{(a' + b')} \tag{9}$$

$$C_t = m_m\xi_1 \tag{10}$$

$$e = \frac{I_m(\xi_2 - \xi_3)}{m_m(b'\xi_2 + a'\xi_3)} \tag{11}$$

where a' and b' are the location of accelerometers from either side of CG (*Refer Fig. 1*) and ξ_1, ξ_2 and ξ_3 are the measured accelerations from the drag, front lift and aft lift accelerometers, respectively. The aerodynamic forces normalized with free stream dynamic pressures $\left(q_\infty = \frac{\gamma}{2}P_\infty M_\infty^2\right)$, flow area ($S$) an base dimension of the model (D_b) can be expressed as;

$$C_d = \left(\frac{N_t \sin\theta + C_t \cos\theta}{q_\infty S}\right) \tag{12}$$

$$C_l = \left(\frac{N_t \cos\theta - C_t \sin\theta}{q_\infty S}\right) \tag{13}$$

$$C_m = \left(\frac{\{C.G. + e\}.N_t}{D_b q_\infty S}\right) \tag{14}$$

The force measurement with accelerometer balance in the hypersonic shock tunnel was first initiated by Vidal (1956) at Cornell Aeronautical Laboratory, New York. Over the past few decades, this balance system has been extensively used for routine measurement of aerodynamic forces over various generic configurations in the hypersonic shock tunnels at Indian Institute of Science (IISc), Bangalore. The initial force measurements over missile configuration, using a three-component accelerometer balance were first reported for three different Mach numbers (Joshi and Reddy 1986; Raju and Reddy 1990). For measuring aerodynamic forces over blunt bodies, additional flares were attached to rear part of model to make it as a lifting body and aerodynamic force coefficients (drag, lift and pitching moment) are then measured with a three-component accelerometer balance (Sahoo 2003; Sahoo *et al* 2003). Other applications include the use of a three-component accelerometer balance to study drag reduction effect of an aerodisc/aerospikes on large angle blunt cones (Viren *et al* 2002). Measurements in hypersonic shock tunnel at various angles of attacks indicated reduction in drag up to 50% with aerodisc/aerospikes. Gas injection at the stagnation point of a blunt cone model to study the effectiveness of film cooling was investigated by measuring drag and surface heating rates simultaneously (Sahoo *et al* 2005). Drag measured on the model with accelerometer balance system showed 27% increase in drag with nitrogen gas injection.

5. STRESS WAVE FORCE BALANCE (SWFB) SYSTEM

Hypersonic steady flows in the test sections are generated for a very short test times in the shock tunnels

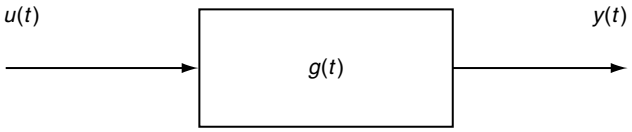

Figure 9. Concept of a stress-wave force balance.

(~ few milliseconds) and still less in expansion tubes (~50 μs). During the short period of steady flow, no steady state force equilibrium can be achieved between the model and its support. When the model is of larger mass and size, the effect of unsteadiness becomes even more severe. For such conditions, it is necessary to include system dynamics to recover time history of aerodynamic force. One such technique, stress wave force balance (SWFB) is proposed at University of Queensland, Australia (Sanderson and Simmons 1991). This principle accepts the fact that no steady state is achieved during the test flow duration. When the aerodynamic load is suddenly applied to the model, stress waves are initiated within the model. These waves propagate and reflect within the model and its support structure. Using system identifications and inverse techniques in the system dynamic analysis, it is possible to determine time history of aerodynamic forces. The details are discussed below.

5.1. Theoretical Background

The aerodynamic forces on a model induce stress waves due to which some strains are developed within the model. If the model and the support structure behave as a linear dynamic system (i.e. the unknown forces that lead to linear strain), then there exists a relationship between the strain (output) and force (input) that causes stress wave activities to induce strain (Fig. 9). Mathematically, the relationship between input and output for a linear system can be expressed as,

$$y(t) = \int_0^t g(t-\tau) \cdot u(\tau) d\tau \tag{15}$$

where $y(t)$ is the strain measured at some point in the model-support structure due to the applied load $u(t)$. The function, $g(t)$ relating the input and output is the characteristics of the structure, known as "transfer function". So, if the system characteristic in the form of impulse response is known, then deconvolution procedure can be applied to determine time history of applied load from the measured strain.

For impulse hypersonic test facilities, the impulse response function can be obtained by measuring the strain history either by a 'step load' or by 'true impulse' during calibration (Mee 2003a). During a 'step load' applied to a system, Laplace transformation can be applied to Eq. (15) to obtain,

$$Y(s) = G(s) \cdot U(s) \tag{16}$$

where $Y(s)$, $G(s)$ and $U(s)$ are the Laplace transforms of $y(t)$, $g(t)$ and $u(t)$ respectively. If the input is of step load of magnitude a, such that,

$$\begin{aligned} u(t) &= 0 \quad t < 0 \\ &= a \quad t \geq 0 \end{aligned} \tag{17}$$

The transfer function for a step load can be obtained as (Mee 2003a),

$$g(t) = \frac{1}{a} \frac{d}{dt} \{ y(t) \} \tag{18}$$

A impulsive force (true impulse) applied to the system in the form of 'delta/Dirac function' is characterized as,

$$u(t) = S \cdot \delta(t) \tag{19}$$

In the above equation, S is the time integral of the pulse and $\delta(t)$ is the unit impulse function defined as,

$$\begin{aligned} \delta(t) &= 0 \quad t \neq 0 \\ &= \infty \quad t = 0 \quad \text{with } \lim_{\varepsilon \to 0} \int_{-\varepsilon}^{\varepsilon} \delta(t)\, dt = 1 \end{aligned} \tag{20}$$

Similarly, the transfer function for an impulsive load can be obtained as (Mee 2003a),

$$g(t) = \frac{y(t)}{S} \tag{21}$$

Thus, it is possible to determine the impulse response function can be determined from the output response for a step load or true impulse as given by Eqs. (18) and (21).

5.2. Measuring Output Response from SWFB

The stress wave force balance is conceived to overcome the restrictions on the model size and mass by accounting the dynamics of the model and support structures with inverse/deconvolution techniques. A single component balance comprises of a model attached to a long sting, known as "stress bar" as shown in Fig. 10. The bar is supported by fine threads in the test section that allows free movement of the model. When the model is subjected to aerodynamic forces, stress waves are initiated that propagate within the model and support structures. In order to detect the stress waves to understand the system dynamics, the strain sensors are mounted on the 'stress bar' close enough to the model. It ensures maximizing the observation time before the onset of complications associated with stress wave reflections comes into existence. The stress bar is long enough such that stress wave reflections from the free end of the stress bar do not reach the strain measurement locations.

There are two types of strain sensors, successfully used in shock tunnels to detect stress waves. They are,

- Semiconductor Strain Gauges
- Piezo-Film Strain Sensor

Semiconductor Strain Gauges: Almost all stiffness dominated force balances discussed earlier use semiconductor strain gauges in wind/shock tunnel testing. Such types of balances are commonly called as "strain gauge force balances". When the measurement is performed in conventional wind tunnel, the useful test time starts when the oscillations are damped down and the force equilibrium is established

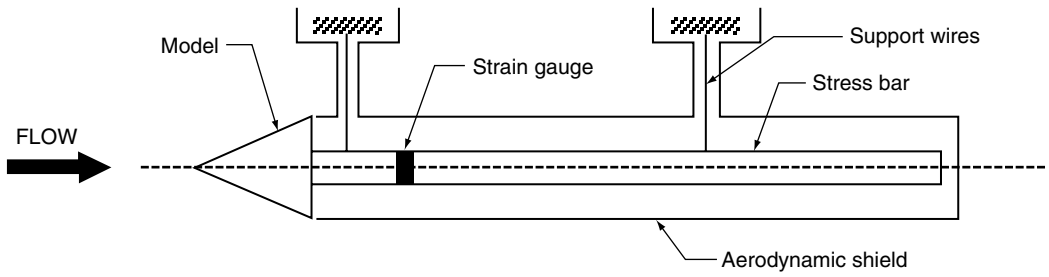

Figure 10. Single component stress-wave force balance (Mee 2003b).

between the balance and loads. The speed of the stress waves in the structure is constant and the system remains steady state. Unlike strain gauge force balance, the interpretation of the strain signal is different in SWFB. Here, the objective is to identify system dynamic response in the form of "transfer function" from a known force-history and corresponding strain gauge response. For shock tunnels, the system dynamics is best understood by a 'step/impulse' load during calibration. The strain response during experiments in shock tunnel is deconvolved with impulse response function to infer complete force history during the test flow.

Piezo-Film Strain Sensors: Dynamic strain gauges made out of piezoelectric polymers (such as, zirconium titanate) are also capable of detecting stress waves (George and James 1968). Such types of sensors are known as "piezofilm strain sensors". In general, there are two broad categories of piezoelectric materials used for preparing the film (Sirohi and Chopra 2000). They are piezoceramics (PZT) and piezoelectric films (PVDF). In PZT category, the most common types include lead zirconate titanates, which are solid solutions of lead zirconate and lead titanate and doped with other elements to obtain specific properties. PVDF is a piezofilm sensor prepared from a polymer (polyvinylidene fluoride). These piezoelectric materials are polarized in character and respond to the forces along a particular axis. The main characteristic of these materials is the utilization of the conserve piezoelectric effect to sense structural deformation when a load is applied. Most of the applications with piezofilm sensors rely on the relative magnitudes of either the voltage or the frequency spectrum of the signal generated by the sensors. In many applications, PVDF sensors are preferred over PZTs because the Young's modulus of PZT materials are comparable to that of aluminium (~72GPa), whereas that of PVDF is approximately $1/12^{TH}$ of that aluminium. Hence, PVDF is less likely to influence the dynamics of the host structure as a result of its own stiffness. Also, PVDF can be used for high temperature applications compared to that of PZT sensors. It has been shown that the response of PVDF sensors is linear and they are effective enough to measure axial stress waves (Smith and Mee 1996a).

5.3. Calibration Methods of SWFB

In order to understand the dynamics of the model and support system in the actual flow environment, it is necessary to know the system characteristics in the form of 'transfer function' as given by Eq. 15. The 'transfer function' is generally obtained for a 'step load' or 'true impulse' for aerodynamic loads in the shock tunnel. There are two major types of calibration experiment performed on the model before it is mounted shock tunnel experiments (Sahoo 2003; Mee 2003b). They are;

- Cut-weight test (for step load)
- Pulse test (for true impulse)

Cut-Wire Calibration Test: Consider the axisymmetric model attached to the long stress bar aligned with the axis of the model (Fig. 10). There are two ways in which a step load can be applied to the model that simulates aerodynamic loading phenomena in the test section. These two situations are schematically shown in Fig. 11. In the first category, a known mass is attached along the axis of the model by fine wire. The balance is supported freely from the other end of the stress bar (Fig. 11-a). In this case, the impulse response derived from step load is valid for the period of time it takes a stress wave to travel from the tip of the model, reflect from the end of the stress bar and return to the strain measurement location. It means, maximum length of the actual signal that could be processed with such an impulse response is limited to this time.

In the second calibration arrangement (Fig. 11-b), the stress wave force balance is again supported vertically, but the load applied to the tip of the model is the weight of the balance system and the other end of the stress bar is free. When the wire is cut, the arrangement experiences a free falling body. Thus, the step response obtained in this case is valid for a longer period time. However, the applied step load is limited by the self weight of the model and stress bar. Sometimes, this arrangement is called "self-weight test".

The output response measured from the strain gauge during cut-weight test is processed by using Eq. 18 to obtain the impulse response for a known 'step load'.

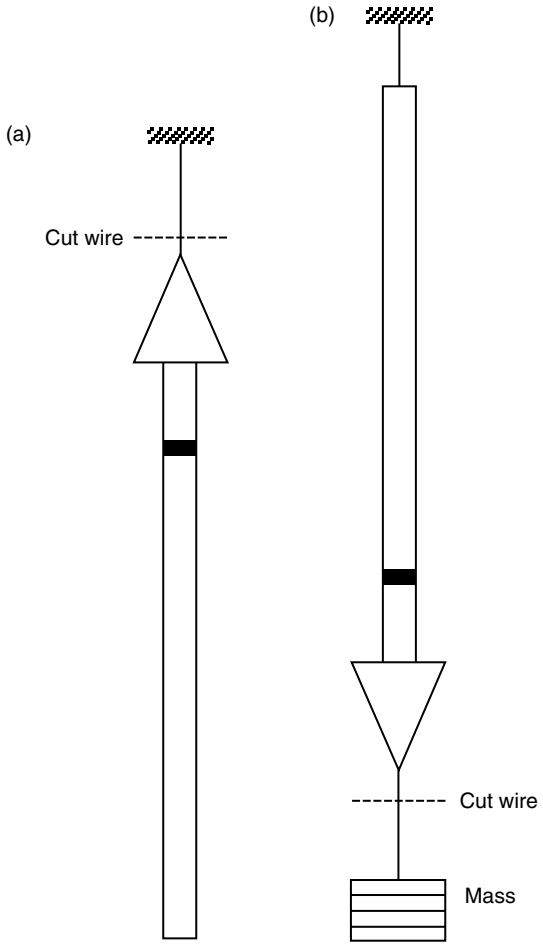

Figure 11 (a & b). Cut-wire calibration test (Mee 2003b).

Pulse Test: This type of test is performed for calibrating a stress wave balance under a "true impulse". It is characterized by sudden load acting for a very short time. In practice, it is almost impossible to achieve a true impulse but a short impulse can be generated that essentially produces same effect as the perfect impulse. This time scale is the characteristics time of the system under test. When the period of the pulse is short, in comparison with the characteristics time of the system, the shape of pulse does not affect the response of the system and only the area under the force-time curve is important (Mee 2003b; Doebelin 1980). However, in longer pulse duration, the response is dependent on the shape of the pulse.

One mechanism for calibrating a stress wave balance system has been reported by applying a short force pulse at a point on the model using an impactor (Mee 2003b). The impactor is instrumented to indicate the time history of force applied during pulse as shown in Fig. 12-a. The another way to apply a short pulse is suspend a small mass (m_b) as a pendulum and allow it to strike the test model as shown in Fig. 12-b. The ball is released from rest from certain initial height, impacts on the model with stress wave force balance, then rebounds and finally comes to rest at certain height, before striking the model second time. Only considering first impact, principle of conservation of momentum and energy can be applied to determine the magnitude of the impulse. Referring to geometry and nomenclature in the Fig. 12-b, the magnitude of impulse (S) may be expressed as (Sahoo 2003; Mee 2003b),

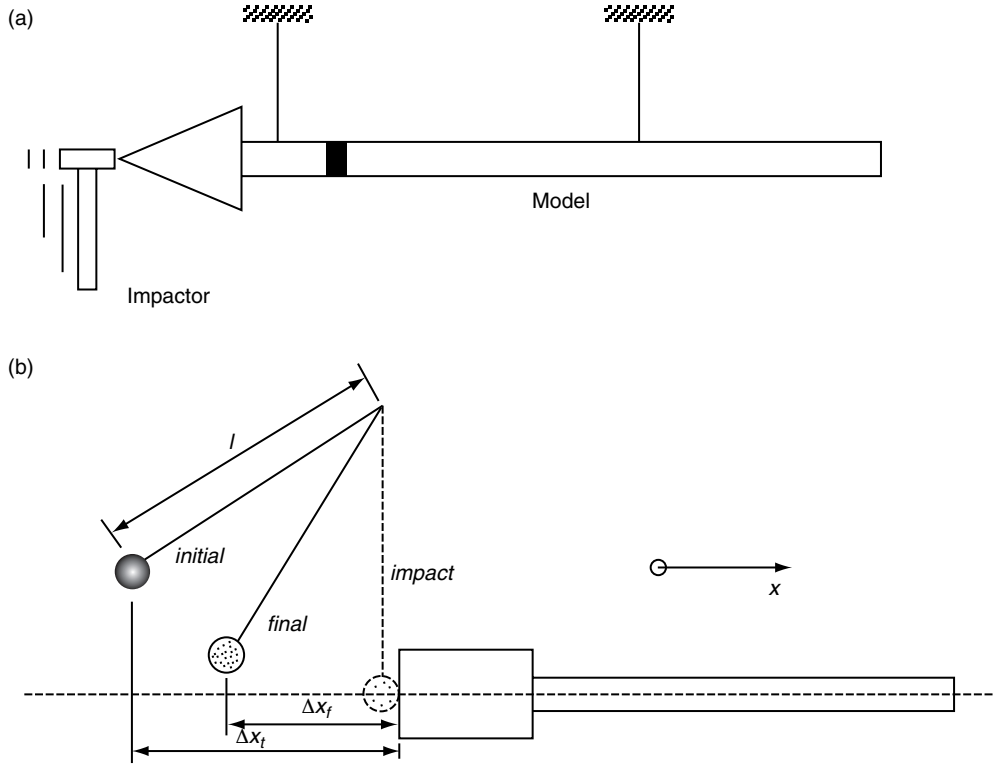

Figure 12 (a & b). True impulse calibration test (Mee 2003b).

$$S = m_b\sqrt{2g}\left(\sqrt{l-\sqrt{l^2-\Delta x_i^2}}+\sqrt{l-\sqrt{l^2-\Delta x_f^2}}\right) \tag{22}$$

The output response measured from the strain sensor during pulse-test is processed by using Eq. 21 to obtain the impulse response for a known true impulse (S).

5.4. Multi-Component Stress Wave Force Balance

A single-component stress wave balance system is mostly desired to measure drag on an aerodynamic body and its success mainly depends on accurate prediction of a single impulse response function during calibration process. When the concept is extended to multiple components, there must be several measured outputs corresponding to unknown inputs. In an ideal situation, each of the measured output is independently related to its corresponding input and can be treated separately for deconvolution for evaluating the impulse response function. However, in a real situation, there is always a coupling present between the individual components (Smith *et al* 2001). For instance, in a balance design to measure lift, drag and pitching moment on a model, a pure drag may produce a signal primarily corresponding drag force output, but it may also give rise to some contributions to other outputs. So, for accurate measurement of all force components, it is essential to determine all impulse responses for all outputs subjected to all inputs. Mathematically, it can be expressed in matrix form for n-component system as (Daniel and Mee 1995; Smith *et al* 2001; Abdel-jawad *et al* 2007),

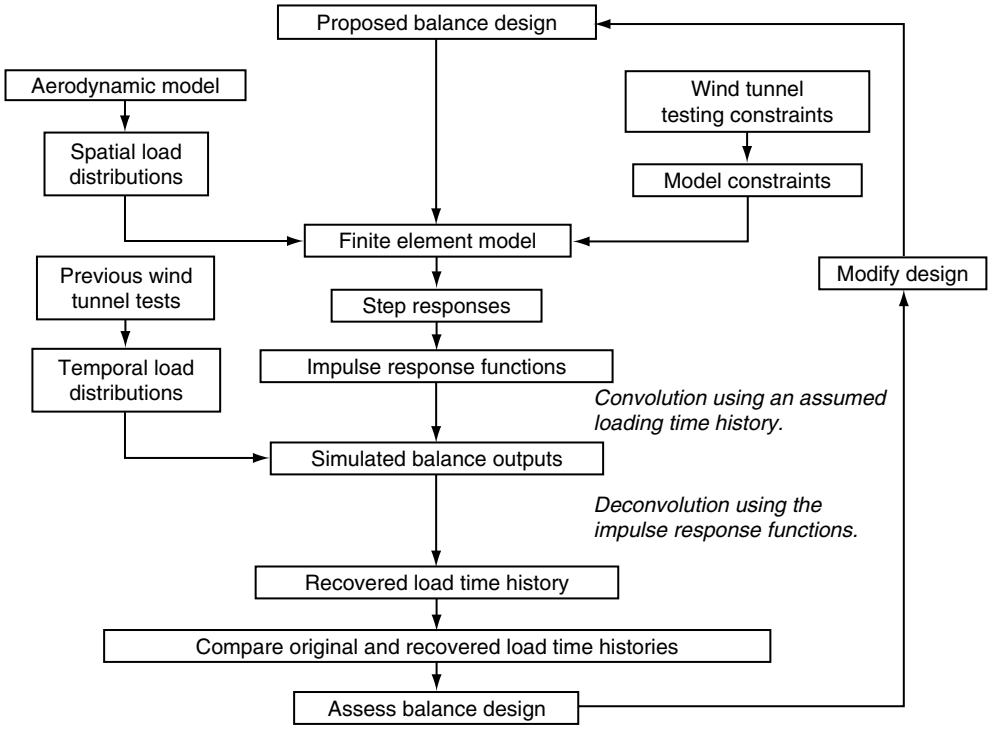

Figure 13. Design methodology for multi-component stress wave force balance (Smith *et al* 2001).

$$\begin{Bmatrix} y_1 \\ y_2 \\ . \\ . \\ y_n \end{Bmatrix} = \begin{bmatrix} G_{11} & G_{12} & ..... & G_{1n} \\ G_{21} & G_{22} & ..... & G_{2n} \\ . & . & ..... & . \\ . & . & ..... & . \\ G_{n1} & G_{n2} & ..... & G_{nn} \end{bmatrix} \begin{Bmatrix} u_1 \\ u_2 \\ . \\ . \\ u_n \end{Bmatrix} \tag{23}$$

where the u_i and y_i are the vectors of the system inputs and outputs, G_{ij} is the impulse response due to each individual components.

In single component balance system, the model-balance system is supported in the test section by a long supporting stress bar supported horizontally from flexible wires. This free-end arrangement is very simple both in terms of calibration and experiments. When a model is to be tested at angle of attack so that effects of lifts, side forces and moments become significant, the free-end arrangement of the stress bar is very complicated and difficult. Sometimes, the size of the test section also limits the model dimension. So, fixed-end support system with short stress-bar is another alternative for mounting the model in the test section at angles of attack. The fixed-end condition is achieved by connecting the end of the supporting stress bar with a relatively large mass, rigidly mounted in the test section. So, the calibration process for a multi-component force balance system mainly relies on exactly replicating the experimental mounting of the model and its support through finite element analysis (Daniel and Mee 1995; Smith *et al* 2001; Abdel-jawad *et al* 2007). The complete design methodology of a multi-component stress wave balance is given in the flow chart (Fig. 13).

5.5. Force Measurement with SWFB

The stress wave force balance was first demonstrated by Sanderson and Simmons (1991) by measuring

drag on a 15° semi-vortex angle cone (200 mm length) in hypervelocity impulse facilities. Resistance strain gauges were used to recover the strain-history and the finite element analysis over the model was used to predict the response function. Subsequently, the drag balances have been developed for various models lengths and tested at different experimental conditions in the shock tunnel (Porter *et al* 1994; Tuttle *et al* 1995). One of the important conclusions in these balances was that the stress wave drag balance could be used on a model in which less than six stress wave reflections might occur within the model during the test period. Further, the concept of single-component stress-wave force balance is extended for measurement of axial force, normal force and pitching moment (Mee *et al* 1996). Experiments performed in the shock tunnel at angles of attack, indicated that forces can be measured satisfactorily within 11% of their theoretical values. Since then, stress-wave force balance system has been routinely used to measure thrust on a scramjet model in the shock tunnel (Robinson *et al* 2004; Robinson *et al* 2006). For hypervelocity flows in expansion tube where the test flow duration is about 50 μs, Smith and Mee (1996b) used a drag balance to measure forces on re-entry capsules. The experiments were conducted in a test flow of partially dissociated carbon-dioxide atmosphere with flow speed of 7 km/s. The drag measurements compared with Modified-Newtonian theory were found to be in good agreement within 11%. Using piezoelectric materials, George and James (1968) used lead zirconium titanate as piezofilm to measure aerodynamic forces on slender body configuration in a shock tunnel for various experimental conditions.

5.6. Accelerometer Balance vs Stress-Wave Force Balance

In order to emphasize the importance of future force measurement techniques in impulse facilities, accelerometer and stress-wave force balance techniques are compared by measuring drag in a shock tunnel (Sahoo 2003). The drag balance comprises of accelerometer, strain gauge and piezofilm mounted on a single model. Some of the aspects of this experiment such as calibration, shock tunnel tests and comparison of results with theory are discussed here.

Test Model and Instrumentation: A 30° semi-apex angle blunt cone with 70 mm base diameter with bluntness (defined as the ratio of nose radius to base radius) 0.85 is fabricated from aluminium. It is attached to a hallow brass sting (stress bar) made out of brass with 11mm diameter and length 555 mm. The mass of the aluminium model and brass sting are 0.14 kg and 0.129 kg, respectively. The sting is instrumented with strain gauges and piezofilms located at a distance 100 mm and 175 mm from the base of the cone as shown in Fig. 14. Two semi conductor strain gauges, each having nominal resistance of 120 Ω and gauge factor of 100 are bonded with their sensitive axes aligned with the axis of the sting. They are connected in a Wheat-stone bridge arrangement and powered with differential amplifier

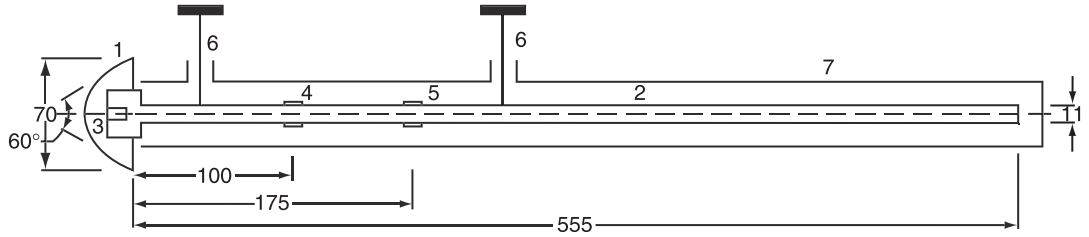

Figure 14. Drag balance instrumented with accelerometer, strain gauge and pieze-film (Sahoo 2003).

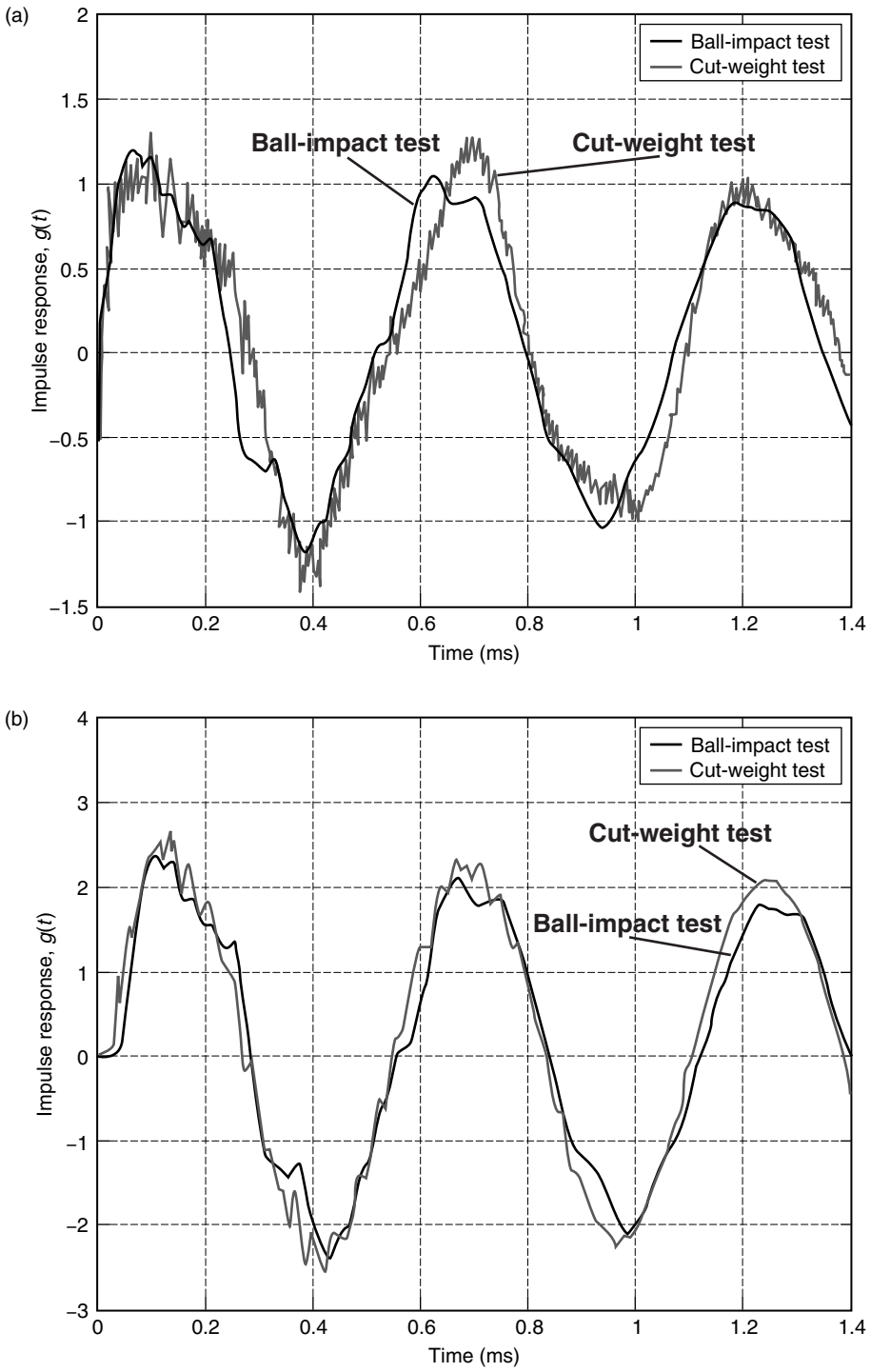

Figure 15. Response function during calibration: (a) strain gauge; (b) piezofilm (Sahoo 2003).

(Ectron Model 560 H) with excitation voltage of 2.5 V. The piezoelectric film made out of polyvinylidene fluoride is wrapped around the circumference of the sting and instrumented with Kistler charge amplifier (Model 566M3). The accelerometer (PCB M303A) is mounted internally along the axis of the model. The sting is suspended by fine threads that ensure free movement of the model. The

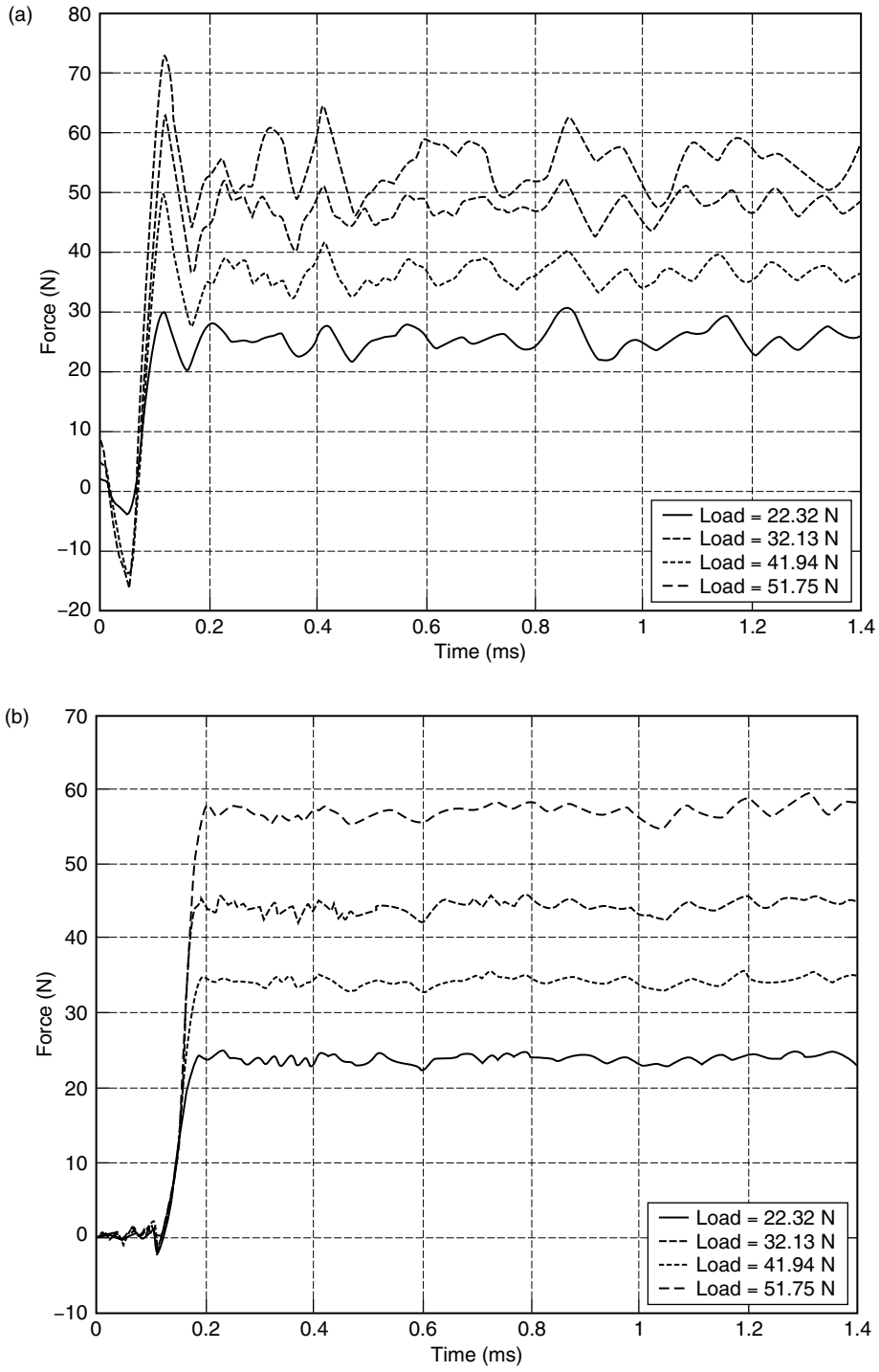

Figure 16. Force history for various cut-wire loads deconvolved with response function of pulse test: (a) strain gauge; (b) piezofilm (Sahoo 2003).

entire drag balance is contained within the aerodynamic shield so that force balance responds only to aerodynamic forces acting on the model.

Measurement with Drag Balance: The strain gauges and piezofilms are calibrated simultaneously by cut-weight test and impact test discussed in the previous sections. Cut-weight tests are performed

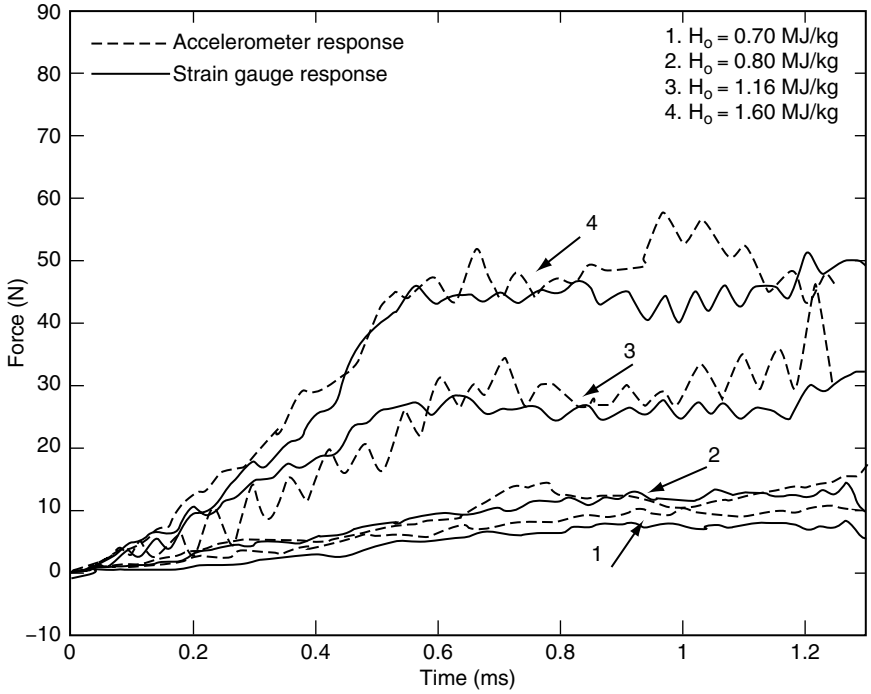

Figure 17. Comparison of force history for shock tunnel tests at different enthalpy conditions (Sahoo *et al* 2005).

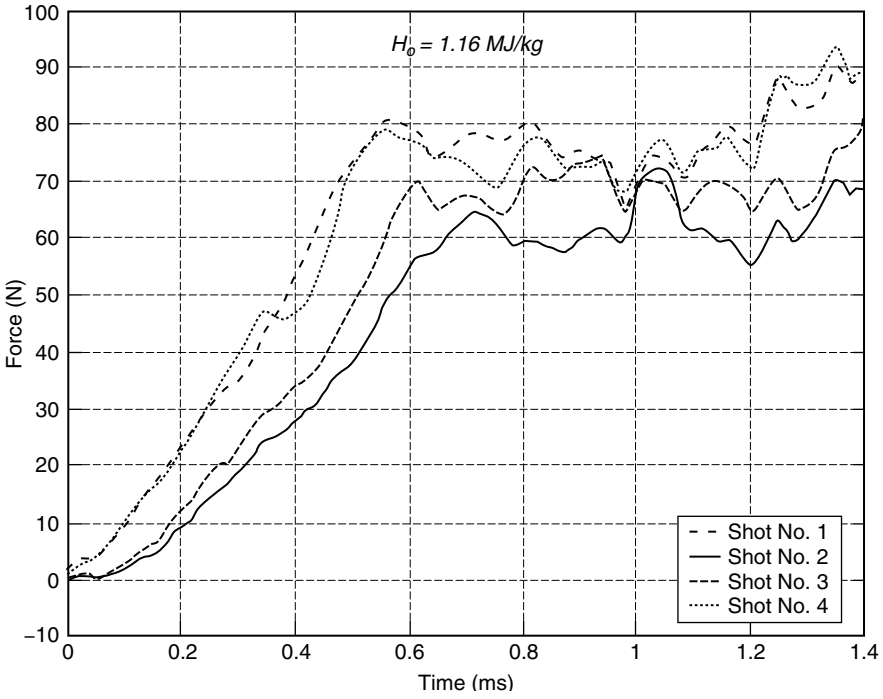

Figure 18. Force history of piezofilms for shock tunnel tests (Sahoo 2003).

with four different loads of 22.3, 32.1, 41.9 and 51.8 N whereas an impulse of 0.0123 N.s is applied to the test model by a pendulous mass. For a known cut-weight load/impulse, the output responses are recorded and the response function is then determined using Eq. 18 (for cut-weight test) and Eq. 21 (for impact test). Various cross-checks are done for comparing the response function obtained from each test (Fig. 15). The force histories for other loads are then inferred by deconvoluting the output response of the strain gauge/piezofilm with the corresponding response function (Fig. 16).

The drag balance is mounted in the shock tunnel to measure drag on the blunt cone model at free stream Mach number 5.75. The typical force-time histories measured by the accelerometer and strain

Table 1. Summary of force measurement techniques in various test facilities

Force Measurement Method	Type of Sensors	Test Facility	Measured Property	Mounting/ Support System	Uncertainty in Aerodynamic Force Coefficient	Major Developments and Future Scope
Inertia dominated balance (Naumann *et al* 1991, 1993)	Accelerometer	Shock tunnel	Displacement of the model during free flight	Free flying technique	±6-9%	Drag, Lift and pitching moment coefficients have been measured successfully
Stiffness dominated balance (Ramesh 2001)	Semiconductor strain gauges	Hypersonic wind tunnel	Strain	Beam element	±3% (during calibration)	Three & Six component balance systems have been reported
Accelerometer balance (Sahoo 2003)	Accelerometer	Shock tunnel	Acceleration history	Flexible rubber	±5-8%	- Single & Three component balance has been tested successfully - Six component balance needs development
				Roller bearing	±9% (for drag force)	Only drag measurement reported and suitable for scramjet drag and thrust measurement
Stress wave force balance (Tuttle *et al* 1995; Mee *et al* 1996)	Semiconductor strain gauge/ piezo film	Shock tunnels, free piston shock tunnel, expansion tube	Strain history	Stress bar (supported in test section by fine threads)	±8-11%	- Drag balance, three component and six component balance have been developed - Very good technology for scramjet force measurement study

gauges for different flow conditions are shown in Fig. 17. The drag forces measured using the accelerometer-based force balance and stress-wave force balance agree closely with each other and well with theoretically estimated values using Newtonian theory (Sahoo *et al* 2005). The force histories measured with piezofilm balance under same flow conditions shows that the drag on the model 2-2.8 times higher in comparison with theoretical values (Fig. 18). It is argued that piezoelectric films are sensitive to dynamic pressures, which may cause this discrepancy in the final results in comparison with the other two standard measurement techniques. However, piezoelectric films show good agreement in calibration tests (Fig. 16-b). This experimental work gives a very good comparison between accelerometer and stress wave balance system. Even though strain gauge is mostly used as strain sensor, but, piezofilms can be also considered as an alternative for shock tunnel applications.

6. CONCLUDING REMARKS

Aerodynamic force measurement in hypersonic flights is necessary for determining many performance and stability parameters. Hypersonic flows are mainly simulated in the laboratory in impulse facilities where the test flow duration is very short (~milliseconds). So, aerodynamic force measurement demands high speed sensors and instrumentation. This review article provides an overall spectrum of two main force measurement techniques namely; accelerometer balance and stress-wave force balance system. The summary of experimental techniques for all class of force balances, covered in this article is given in Table 1. In most of the reported literatures on accelerometer, the measurement is limited to drag and/or lift and pitching moment.

Till date, the main focus on accelerometer balance system is to measure drag on the various generic models. However, effects of support system on lift and moments need further study. Again, the size of the model is one of the issues because the system dynamics will be different for a large-sized model and several accelerometers might be needed for complete information of the model accelerations. Secondly, for measuring forces at angles of attack, the combined effects of forces must be taken into account while inferring model accelerations. A three-dimensional finite modelling can open a new direction of research to design and develop a six-component accelerometer balance system for impulse facilities. Accordingly, the tri-axial accelerometers can be selected to infer complete set of information of the forces. Sleek design, easy operation and direct measurement of model acceleration are some of the advantages of this balance system. So, accelerometer balance system holds a very promising future for recent years.

The importance of SWFB is realized when the size and mass of the model is relatively high because the period of lowest frequency of the force balance is of the similar order to the duration of test flow. Unlike accelerometer balance, it is not possible to eliminate the damping effects completely. SWFB technique uses system identification and inverse technique in the analysis of force balance signal. However, the accuracy of this balance system mainly depends on the exhaustive calibration process. Calibration methods such as cut-weight test and pulse test can be used very accurately for drag balances. When the force measurements are extended for lifts and moments, exhaustive finite element formulation is necessary for the entire support system in the way, it is mounted in the test section of the tunnel. Main advantage of this technique is that it takes into account the system dynamics in interpreting the force history. The future direction of research should focus on multi-component force measurement system that covers the entire spectrum in the design of hypersonic vehicles.

REFERENCES

[1] Abdel-jawad MM, Mee DJ and Morgan RG (2007) New calibration technique for multi-component stress wave force balances, Review of Scientific Instruments, 78: 1–7.

[2] Anderson JD Jr (2006) Hypersonic and High-Temperature Gas Dynamics, AIAA Education Series; Ed: J.A. Schetz, Second Edition, American Institute of Aeronautics and Astronautics, Virginia.

[3] Ardasheva MM, Nevskii LB and Pervushin GE (1985) Measurement of pressure distribution by means of indicator coating, Journal of Applied Mechanics and Technical Physics 26(4): 469–474.

[4] Bathe KJ (1997) Finite Element Procedures, Prentice-Hall of India Private Limited; New Delhi.

[5] Bernstein L (1975) Force measurements in short-duration hypersonic facilities, AGARDograph 214.

[6] Bernstein L and Stott GT (1982) A laser-interferometric trajectory-following system for determining forces on a freely flying models in a shock tunnel, 13TH International Symposium on Shock Waves and Shock Tubes, Niagara Falls, New York.

[7] Bertin JJ and Cummings RM (2003) Fifty years of hypersonics; where we've been, where we're going, Progress in Aerospace Sciences, 39: 511–536.

[8] Carbonara M (1993) Aerodynamic force measurements in the VKI Longshot Hypersonic Facility, New Trends in Instrumentation for Hypersonic Research: Ed. A. Boutier, NATO ASI Ser. E, 224: 317–325.

[9] Charles EW and Merle RW (1962) Heat transfer to slender cones in hypersonic air flow including effects of the yaw and nose bluntness, Journal of Aerospace Sciences, 29(7): 761–774.

[10] Dale G, Baust H, Tyler C, Jordan J, Weaver W and Clinehens G (1998) Pressure sensitive paint measurements in very low-speed flows, Proceedings of Sixth Annual Pressure Sensitive Paint Workshop, The Boeing Company, Seattle, Washington, October 06-08 ; 16–1 to 16–6.

[11] Daniel WJT and Mee DJ (1995) Finite element modelling of a three-component force balance for hypersonic flows, Computers and Structures 54(1); 35–48.

[12] Doebelin EO (1980) System Modelling and Response: Theoretical and Experimental Approaches, John Wiley and Sons, New York.

[13] Doolan CJ and Morgan RG (1999) A two-stage free-piston driver, Shock Waves 9: 239–248.

[14] East RA and Hillier TJ (1985) Free-flight oscillatory experiments in a hypersonic gun tunnel, 15TH International Symposium on Shock Waves and Shock Tubes, Berkeley CA.

[15] Gallery J, Gouterman M, Callis J, Khalil G, McLachlan BG *et al* (1994) Aerodynamic temperature measurements by luminescence imaging, Review of Scientific Instruments 65(3); 712–720.

[16] George RD and James FM (1968) An improved piezo-electric balance for aerodynamic force measurement, IEEE Transactions on Aerospace and Electronics System, AES-4 (3): 351–359.

[17] Holden MS (1985) Experimental studies of the effects of axi-symmetric transition on the aero-thermal characteristics of hypersonic blunted slender cones, AIAA Paper 85–0325 (1985).

[18] Houck SW, Hepp RG, Morris MJ and Benne ME (1996) Pressure sensitive paint flight test, IEEE Aerospace Applications Conference, Aspen Co, February 03-10; 4: 241–252.

[19] Hubner JP, Carroll BF, Schanze KS and Ji HF (2000) Pressure-sensitive paint measurements in a shock tube, Experiments in Fluids 28: 21–28.

[20] Hubner JP, Carroll BF, Schanze KS, Ji HF and Holden MS (2001) Temperature and pressure-sensitive paint measurements in short-duration hypersonic flow, AIAA Journal, 39(4): 654–659.

[21] Itoh K, Komuro T, Sato K, Tanno H and Ueda S (2001) Hypersonic aerodynamic research of HOPE using high enthalpy shock tunnel, AIAA Paper 01–1824.

[22] Jessen C and Gronig H (1989) A new principle for short duration six component balance, Experiments in Fluids 8: 231–233.

[23] Joarder R and Jagadeesh G (2004) A new free floating accelerometer balance system for force measurements in shock tunnels, Shock Waves 13: 409–412.

[24] Joshi MV and Reddy NM (1986) Aerodynamic force measurements over missile configurations in IISc shock tunnel at M_∞ = 5.5, Experiments in Fluids 4: 338–340.

[25] Jules K, Carbonaro M and Zemsch S (1995) Application of pressure sensitive paint in hypersonic flows, NASA TM-106824.

[26] Lam LY and Stollenwerk J (1966) Aerodynamic force measurement of free-flight models in a hypervelocity shock tunnel, AIAA Paper 66–771.

[27] Lu FK and Wilson DR (1994) Survey of short duration, hypersonic and hypervelocity facilities, AIAA Paper 94–2491.

[28] Marqart EJ and Coulter SM (1998) Impulse measurement technology development at Arnold Engineering Development Center (AEDC), AIAA Paper 98–203.

[29] McDevitt JB and Larson HK (1966) A technique for launching free-flying models in conventional wind tunnels, AIAA Paper 66–773.

[30] McLachlan BG, Bell JH, Kennelly RA, Schreiner JA, Smith SC *et al* (1992) Pressure sensitive paint for use in supersonic high-sweep oblique wing (SHOW) test, AIAA Paper 92–2686.

[31] McLachlan BG, Bell JH, Espina JH, Gallery J, Gouterman M *et al* (1992a) Flight testing of a luminescent surface pressure sensor, NASA TM-103970.

[32] Mee DJ, Daniel WJT and Simmons JM (1996) Three component force balance for flows of milliseconds duration, AIAA Journal 34(3): 590–595.

[33] Mee DJ (2003a) Dynamic calibration of force balances for impulse hypersonic facilities, Shock Wave 12: 443–455.

[34] Mee DJ (2003b) Dynamic calibration of force balances, Research report number 2002/6, Department of Mechanical Engineering, University of Queenland, Australia.

[35] Modarress D and Azzazy M (1988) Modern experimental techniques for high speed flow measurements, AIAA Paper 88–0420.

[36] Naumann KW, Ende H and Mathieu G (1991) Techniques for aerodynamic force measurement within milliseconds in shock tunnel, Shock Wave, 1: 223–232

[37] Naumann KW, Ende H, Mathieu H and George A (1993) Millisecond aerodynamic force measurement with side-jet model in the ISL shock tunnel, AIAA Journal 31(6): 1068–1074.

[38] Platou AS (1968), The wind tunnel free flight testing technique, AIAA Paper 68–388.

[39] Porter IM, Paull A, Mee DJ and Simmons JM (1994) Shock tunnel measurements of hypervelocity blunted cone drag, AIAA Journal 32(12): 2476–2477.

[40] Ramesh R (2001) Thin flat balances for testing thin delta wings at hypersonic speeds, Measurement Science and Technology 12: 1555–1567.

[41] Raju C and Reddy NM (1990) Aerodynamic force measurements over missile configurations in IISc shock tunnel at M_∞ = 3.85 and 9.15, Experiments in Fluids, 10: 175–177.

[42] Robinson MJ, Mee DJ, Tsai CY and Bakos RJ (2004) Three-component force measurements on a large scramjet in a shock tunnel, Journal of Spacecraft and Rockets, 41(3): 416–425.

[43] Robinson MJ, Mee DJ and Paull A (2006) Scramjet lift, thrust and pitching moment characteristics measured in a shock tunnel, Journal of Propulsion and Power, 22(1): 85–95.

[44] Rogers CE and Mason RP (1966) Some recent advances in short-duration aerodynamic testing techniques, AIAA Paper 66–762.

[45] Sahoo N (2003) Simultaneous measurement of aerodynamic forces and convective surface heat transfer rates for large angle blunt cones in hypersonic shock tunnel, PhD Thesis, Indian Institute of Science, Bangalore, India.

[46] Sahoo N, Mahapatra DR, Jagadeesh G, Gopalakrishnan S and Reddy KPJ (2003) An accelerometer balance system for measurement of aerodynamic force coefficients over blunt bodies in a hypersonic shock tunnel, Measurement Science and Technology, 14: 260–272.

[47] Sahoo N, Kulkarni V, Saravanan S, Jagadeesh G and Reddy KPJ (2005) Film cooling effectiveness on a large angle blunt cone flying at hypersonic speed, Physics of Fluids 17(3): 1–11.

[48] Sahoo N, Suryavamshi K, Reddy KPJ and Mee DJ (2005) Dynamic force balances for short-duration hypersonic testing facilities, Experiments in Fluids 38: 606–614.

[49] Sahoo N, Mahapatra DR, Jagadeesh G, Gopalakrishnan S and Reddy KPJ (2007) Design and analysis of a flat accelerometer based force balance for shock tunnel testing, Measurement, 40 (1): 93–106.

[50] Sanderson SR and Simmons JM (1991) Drag balances for hypervelocity impulse facilities, AIAA Journal, 29(12): 2185–2191.

[51] Simmons JM (1995) Measurement techniques in high-enthalpy hypersonic facilities, Experimental Thermal and Fluid Science, 10: 454–469.

[52] Sirohi J and Chopra I (2000) Fundamental understanding of piezoelectric strain sensors, Journal of Intelligent Material Systems and Structures 11: 246–257.

[53] Smith AL and Mee DJ (1996a) Dynamic strain measurement using piezoelectric polymer film, Journal of Strain Analysis for Engineering Design 31(6): 463–465.

[54] Smith AL and D.J. Mee (1996b), Drag measurements in a hypervelocity expansion tube, Shock Waves 6(3): 161–166.

[55] Smith AL, Mee DJ, Daniel WJT and Shimoda T (2001) Design, modelling and analysis of a six-component force balance for hypervelocity wind tunnel testing, Computers and Structures, 79: 1077–1088.

[56] Stalker RJ, Paull A, Mee DJ, Morgan RG and Jacobs PA (2005), Scramjets and shock tunnels – The Queeensland experience, Progress in Aerospace Sciences, 41: 471–513.

[57] Storkmann V, Olivier H and Gronig H (1998) Force measurement in hypersonic impulse facilities, AIAA Journal, 36(3): 342–348.

[58] Strawa AW, Chapman GT, Canning TN and Arnold JO (1991) Ballistic range and aerothermodynamic testing, Journal of Aircraft, 28(7): 443–449.

[59] Tuttle SL, Mee DJ and Simmons JM (1995) Drag measurement at Mach 5 using a stress wave force balance, Experiments in Fluids 19(5): 336–341.

[60] Van Dyke MD (1958) The supersonic blunt body problem – Review and extension, Journal of Aerospace Sciences, 25: 485–496.

[61] Vidal RJ (1956) Model instrumentation techniques for heat transfer and force measurements in a hypersonic shock tunnel, Cornell Aeronautic Laboratory Report WADC TN 56–315.

[62] Viren M, Saravanan S and Reddy KPJ (2002) Shock tunnel study of spiked aerodynamic bodies flying at hypersonic Mach number, Shock Wave 12: 197–204.

[63] Wyborny W and Requardt G (1974) A new aerodynamic free flight testing system for six-component measurements in short duration wind tunnels, AIAA Paper 74–613.